CPP

Contributions to Plasma Physics

www.cpp-journal.org

WILEY-VCH

REPRINT

Contrib. Plasma Phys. **52**, No. 3, 224 – 228 (2012) / **DOI** 10.1002/ctpp.201100085

Proton Crystallization in a Dense Hydrogen Plasma

V. S. Filinov[1]*, **M. Bonitz**[2], **H. Fehske** [3], **V. E. Fortov**[1], and **P. R. Levashov**[1]

[1] Joint Institute for High Temperatures, Russian Academy of Sciences, Izhorskaya 13, bd. 2, 125412 Moscow, Russia

[2] Institute for Theoretical Physics and Astrophysics, Christian Albrechts University Kiel, Leibnizstrasse 15, D-24098 Kiel, Germany

[3] Institute of Physics, University Greifswald, Felix-Hausdorff-Str. 6, D-17487 Greifswald, Germany

Received 14 October 2011, revised 16 February 2012, accepted 23 February 2012
Published online 11 April 2012

Key words Strongly correlated two-component plasma, Coulomb crystallization.

We perform a first-principle analysis of Coulomb crystallization in neutral two-component mass asymmetric plasmas by large-scale path integral Monte Carlo simulations for a dense hydrogen plasma in a broad density range. We observe two large jumps in the relative distance fluctuations of protons that are connected with qualitative changes in the behavior of the proton pair distribution function and are attributed to the formation of a spatially ordered state. A third smaller jump inside the ordered phase indicates a structural transition.

1 Introduction

In a recent letter [1] we proved that in a two-component (electron and proton) dense hydrogen plasma at sufficiently low temperatures and high densities the protons will spontaneously order by forming a Coulomb crystal embedded in a highly degenerate electron gas (for an overview on Coulomb crystallization see e.g. [2]). A simplified description of this system is given by the one-component plasma (OCP) model consisting of positive charges (protons for example) in an uniform (rigid) neutralizing background of electrons. For the classical OCP extensive studies, based on molecular dynamics and analytical approaches, have revealed the following regimes: a proton gas (plasma) state for coupling parameter (CP) less than one; a proton liquid state or proton glass state if CP exceeds one; and finally, for still larger CP (≥ 175 in three dimensions), a proton crystal state, for a review see e. g. [3]. Thermodynamically, the glassy state is metastable.

In order to localize structural transitions between different states of matter various criteria have been used in the literature, thereof many based on the analysis of the pair distribution functions (PDF). For example a jump of the height of the first PDF peak was observed at freezing in a macroscopic 2D OCP, see [4] and references therein. Unfortunately, in simulations with a limited particle number—as unavoidable in quantum MC simulation of fermions—the height and shape of the peaks in the PDF are sensitive to the size of Monte Carlo cell and the number of particles in it. Additional difficulties arise from the possible existence of metastable states. To overcome these difficulties we follow the idea of Lindemann [5] and analyze the fluctuations of nearest neighbor distances of the system for different states of matter. According to Lindemann [5] an increased amplitude of the vibrations of the particles around their equilibrium positions is the physical reason for the melting of the crystal. If the vibrational amplitude becomes so large that particles start to invade the space of their nearest neighbors the melting process sets in. At the melting point the root mean square vibration amplitude $\sqrt{< u^2 >}$ exceeds a threshold value of about $10\% - 28\%$ of the nearest neighbor distance $\bar{r}$, depending on the type of pair interaction, dimensionality and spin statistics [2]. In general, phase transitions between different states of matter and structural transitions within the solid phase are indicated by sharp jumps in the relative distance fluctuations between neighboring particles. Therefore, in this paper we will analyze such jumps in order to localize structural transitions in a dense two-component hydrogen plasma.

* Corresponding author. E-mail: vladimir_filinov@mail.ru, Phone: + 7 495 931-0719, Fax: + 7 495 485-7990

As mentioned before, charge crystallization was confirmed for OCP models with Coulomb and Yukawa interactions [6, 7] by early two-component path integral Monte Carlo (PIMC) simulations [8]. In Ref. [1] the general conditions for the stability of such an ionic crystal in neutral two-component Coulomb systems were derived starting from a one-component plasma (OCP) model and, in particular, the critical mass ratio M (between the heavy positive and light negative charges) for Coulomb crystallization was found to be around 80 in three dimensions; see also Ref. [9]. In this contribution we discuss the phase diagram of a neutral two-component mass asymmetric plasma without the assumption of a rigid background. To this end we perform extensive direct PIMC simulations of a macroscopic spatially homogeneous fully ionized two-component electron-proton plasma in thermodynamic equilibrium and determine the temperature and density range of proton crystallization from first principles. Our results are of importance for the fundamental understanding of nonideal plasmas [10–12], with direct relevance for dwarf stars, laser-cooled expanding plasmas, and laser plasmas [13].

2 Model and Method

We consider a neutral two-component Coulomb system consisting of $N_e = N_p = N$ electrons and protons in equilibrium. Its Hamiltonian, $\hat{H} = \hat{K} + \hat{U}$, contains kinetic ($\hat{K}$) and Coulomb interaction energy ($\hat{U} = \hat{U}_{pp} + \hat{U}_{ee} + \hat{U}_{ep}$) parts. Within a canonical ensemble, the thermodynamic properties of the system are fully described by the density operator $\hat{\rho} = e^{-\beta\hat{H}}/Z$ with the partition function Z, at fixed volume V and inverse temperature $\beta = 1/k_BT$, given by

$$Z(N_e, N_p, V; \beta) = \frac{1}{N_e!N_p!} \sum_\sigma \int_V dq\, \rho(q, \sigma; \beta), \tag{1}$$

where $\rho(q, \sigma; \beta)$ denotes the diagonal matrix elements of the density operator for total spin value σ. In Eq. (1), $q = \{q_e, q_p\}$ and $\sigma = \{\sigma_e, \sigma_p\}$ denote the spatial coordinates and spin degrees of freedom of electrons and protons, i.e. $q_a = \{q_{1,a} \dots q_{l,a} \dots q_{N_a,a}\}$ and $\sigma_a = \{\sigma_{1,a} \dots \sigma_{l,a} \dots \sigma_{N_a,a}\}$, with $a = e, p$. Of course, the exact density matrix of such an interacting quantum systems is not accessible, in particular not for low temperatures and high densities. It can be approximately constructed, however, using a path integral approach [14–17] based on the operator identity $e^{-\beta\hat{H}} = e^{-\Delta\beta\hat{H}} e^{-\Delta\beta\hat{H}} \dots e^{-\Delta\beta\hat{H}}$, where $\Delta\beta = \beta/(n+1)$. It allows us to rewrite the integral in Eq. (1) as

$$\begin{aligned} \sum_\sigma \int dq^{(0)}\, \rho(q^{(0)}, \sigma; \beta) \;&=\; \int dq^{(0)} \dots dq^{(n)}\, \rho^{(1)} \cdot \rho^{(2)} \dots \rho^{(n)} \\ &\times \sum_\sigma \sum_{P_e} \sum_{P_p} (-1)^{\kappa_{P_e} + \kappa_{P_p}}\, \mathcal{S}(\sigma, \hat{P}_e\hat{P}_p\sigma'_a) \times \hat{P}_e\hat{P}_p \rho^{(n+1)}\big|_{q^{(n+1)} = q^{(0)}, \sigma' = \sigma}. \end{aligned} \tag{2}$$

Here the spin gives rise to the spin part of the density matrix ($\mathcal{S}$) which accounts for exchange effects due to the permutation operators $\hat{P}_e$ and $\hat{P}_p$ acting on the electron and proton coordinates $q^{(n+1)}$ and spin projections σ', respectively. In Eq. (2), the sum is over all permutations with parity κ_{P_e} and κ_{P_p}. The index $k = 1 \dots (n+1)$ labels the off-diagonal high-temperature density matrices $\rho^{(k)} \equiv \rho\left(q^{(k-1)}, q^{(k)}; \Delta\beta\right) = \langle q^{(k-1)}|e^{-\Delta\beta\hat{H}}|q^{(k)}\rangle$. Accordingly each particle is represented by a set of $(n+1)$ coordinates (beads), i.e. the whole particle configuration is represented by a $3(N_e+N_p)(n+1)$–dimensional vector $\tilde{q} \equiv \{q_{1,e}^{(0)}, \dots q_{1,e}^{(n+1)}, q_{N_e,e}^{(0)} \dots q_{N_e,e}^{(n+1)}; q_{1,p}^{(0)} \dots q_{N_p,p}^{(n+1)}\}$. The approximation for the high-temperature density matrices involves effective quantum pair Kelbg potentials for the interaction between beads with the same indices (for details see [9, 15, 16]).

3 Numerical results and discussion

For the actual three-dimensional PIMC simulations of the dense hydrogen plasma we treat two hundred particles (each represented by twenty beads) in the MC cell and apply periodic boundary conditions. In what follows we use atomic units, i.e. lengths are measured in units of the Bohr radius a_B and the density is given in units of the Brueckner parameter $r_s = \bar{r}/a_B$, where $\bar{r}$ is the average interparticle distance. Fig. 1 shows snapshots of the PIMC simulations of a fully ionized ion-electron plasma with different mass ratios. We observe an decreasing

extension of the positive charge wave functions with increasing mass ratio M, which is responsible for quantum melting of the Wigner ion crystal if M falls blow the critical value (left panel). Note that for both shown cases, $M = 50$ and $M = 800$, the electrons are in a degenerate Fermi gas state.

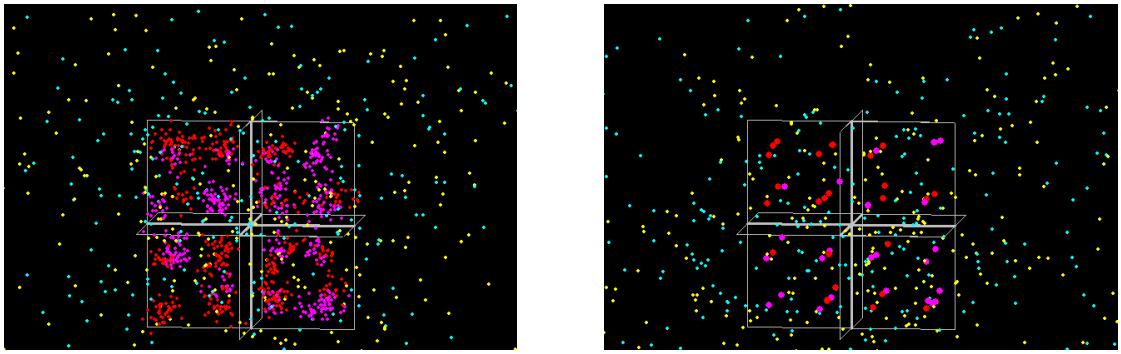

Fig. 1 Snapshots of the PIMC simulations of a fully ionized electron-ion plasma with mass ratio $M = 50$ (left) and $M = 800$ (right) at the same density and temperature indicating the mass-dependent quantum melting of the ion crystal. The ions are shown by red and pink clouds of dots corresponding to spin up and spin down ions, respectively. Likewise electrons are represented by clouds of yellow and blue dots.

As emphasized in the introduction, for a quantitative analysis of structural transitions in a dense hydrogen plasma one has to determine the relative distance fluctuations of protons (RD-PP) $\sqrt{< u^2 >}/\bar{r}$. To get deeper physical insight into the behavior of the RD-PP, we consider the proton–proton pair distribution function (PP-PDF) defined as

$$g_{ab}(|r_{1,a} - r_{1,b}|) = \frac{N_e! N_p!}{Z} \sum_{\sigma} \int_V dq\, \delta(r_{1,a} - q_{1,a})\, \delta(r_{2,b} - q_{2,b})\, \rho(q, \sigma; \beta)\,. \tag{3}$$

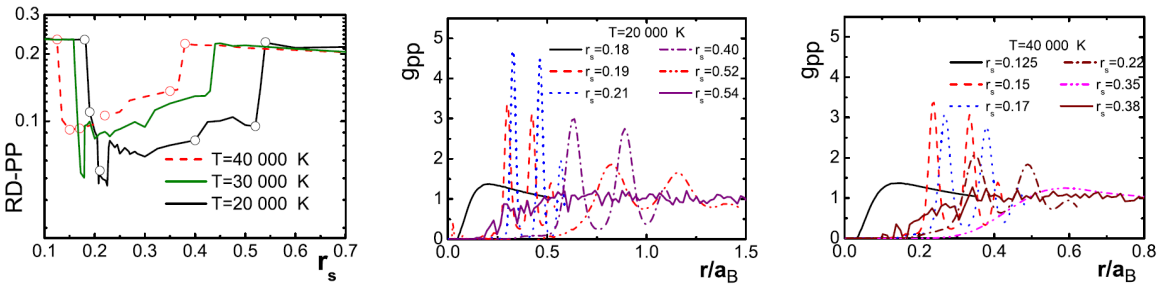

Fig. 2 Left panel: Relative proton-proton distance fluctuations for three temperatures. Sharp jumps signal structural transitions. For $T = 20\,000$ K: left jump – from a degenerate disordered phase of protons ($r_s \approx 0.18$) to an ordered phase ($r_s \approx 0.2$); middle jump – structural transition inside the ordered phase ($r_s \approx 0.225...0.23$); right jump – from a proton ordered phase ($r_s \approx 0.52$) to a disordered phase ($r_s \approx 0.53$). Similar behavior is observed for $T = 30\,000$ K. For $T = 40\,000$ K the jump in the ordered phase is missing. Middle and right panels: Proton-proton pair distribution functions for a fully ionized hydrogen plasma with $M = 2000$ at various particle densities at $T = 20\,000$ K (middle) and $40\,000$ K (right).

Figures 2 and 3 give the results of our PIMC calculations for three characteristic temperatures for which we observe different phases. The left panel of figure 2 illustrates the behavior of the RD-PP as a function of the mean interparticle distance. At high densities ($r_s \leq 0.18$) and $T = 20.000$ K, RD-PP is practically constant. In this region the PP-PDF is approximately equal to one, except for the correlation hole at very small distances, which is characteristic for a weakly coupled degenerate gas of protons (see middle panel of Figure 2). When the density is decreased to $r_s \approx 0.2$ a sudden jump of the RD-PP occurs, which is related—as can be concluded from the change of the PP-PDF—to a transition to a perfect proton crystal. At $r_s \approx 0.2$, g_{pp} exhibits well pronounced

narrow peaks and dips; cf. the middle panel of Figure 2. Thus, in the density interval from $r_s = 0.2$ to $r_s = 0.23$ protons are ordered in a crystal-like structure.

A further density decrease ($r_s \geq 0.23$) results in a second sharp jump of the RD-PP with smaller magnitude. This jump is accompanied by a broadening and lowering of the peaks of the PP-PDF. As yet, the nature of the resulting state is not fully understood from the available data. a possible explanation is that the system is in another (metastable) crystalline state which vanishes only at $r_s = 0.52$ where a third large jump is found. Another possibility is that we observe a phase transition to a liquid-like state that persists until $r_s = 0.52$. As the density is further reduced to $r_s = 0.54$, the RD-PP shows another large jump while the PP-PDF changes dramatically to a shape typical for a weakly coupled plasma. While the behavior of the RD-PP along the second isotherm $T = 30.000$ K is very similar, the third isotherm, $T = 40.000$ K, does not exhibit the intermediate smaller jump indicating that the ordered phase remains homogeneous throughout the density interval from $r_s = 0.15$ to 0.35.

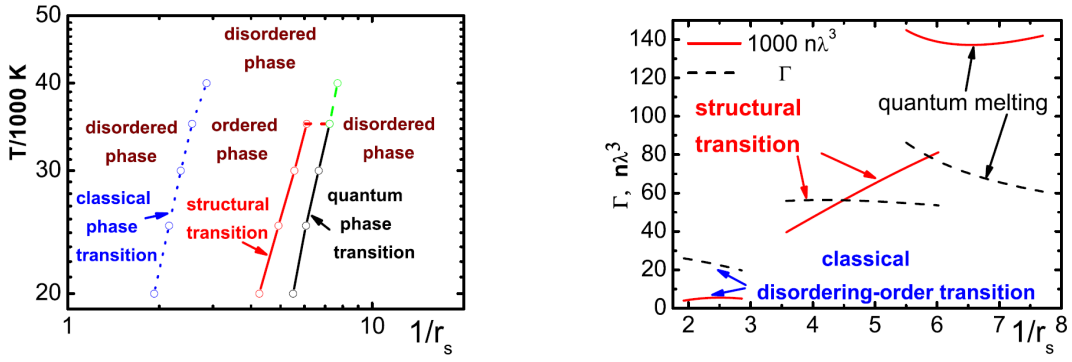

Fig. 3 Left panel: Hydrogen phase diagram in the vicinity of proton crystallization. Lines with circles are PIMC simulation results. The ordered phase with low values of the RD-PP is embedded into classical and quantum disordered phases, appearing to the left of the blue line and right of the black line, respectively. The red line indicates a structural transition inside the ordered phase. The ordered proton phase terminates in a triple point. Right panel: Values of the classical coupling parameter Γ (black dashed lines) and quantum degeneracy parameter $n\lambda^3$ (red full lines) along the three lines along which the RD-PP have a jump, cf. the left panel.

Our PIMC results for the PP-PDF and RD-PP are summarized in the phase diagram, cf. left panel of figure 3 (see lines with circles). An increase of the density, at fixed temperature, first leads to a Mott transition from a neutral plasma (consisting of atoms and molecules) to a fully ionized disordered gas-like plasma. This transition is not shown in the phase diagram as related $r_s \approx 1.5 - 2$. Upon further compression the sharp jump of the RD-PP indicates a transition to a spatially ordered state (blue dotted line). The broad region of smooth variation of the RD-PP indicates that this state persists over a broad density interval. For temperatures below $40.000K$ a further increase of the density leads to a further reduction of the RD-PP, signaling another ordering transition of protons. At a slightly higher density the RD-PP jumps up again when the melting of the proton crystal into a proton quantum disordered phase takes place as a consequence of overlapping proton wave functions. At temperatures larger than $40.000K$ the second jump of the RD-PP is missing. The characteristic values of the coupling parameter Γ and degeneracy parameter $n_p\lambda_p^3$ along the three phase boundaries are presented in the right panel of Fig. 3. Here $\lambda_p^2 = 2\pi\hbar^2/(mk_BT)$ is the thermal proton DeBroglie wave length squared. We find that Γ is of the order of $23, 60$ and 80, respectively, whereas the proton degeneracy parameter at these phase boundaries is of the order of $0.01, 0.06$ and 0.14, respectively.

To summarize, we presented first simulation results for the phase diagram of a two-component dense quantum plasma in the vicinity of the proton crystal. Note that these simulations differ qualitatively from previous OCP results. Here we do not assume a rigid electron background and fully allow for a nonuniform electron density due to the interaction with the proton potential field. We like to emphasize that some of these results are still preliminary, in particularly the interpretation of the ordered phase in between the two large jumps of the RD-PP is not yet fully understood. Whether this whole density interval is characterized by a proton solid which undergoes several structural transitions at high densities or whether the proton crystal phase exists only in the narrow region of the lowest values of the RD-PP requires further analysis.

Our findings differ substantially from earlier predictions based on the OCP model: (i) In the classical part of the phase diagram the crystal appears to be stabilized as compared to the OCP prediction, we find a nearly constant coupling parameter Γ^{cr} around 23 (60) at the disorder-order transition (at the structural transition inside the ordered phase); (ii) In the quantum part of the phase diagram the crystal is destabilized compared to the OCP prediction of $r_s^{cr} = 100$ and vanishes at lower densities, also, the quantum melting temperature increases with density, in contrast to the OCP. Thus we arrive at the conclusion that the simplified OCP treatment of the liquid-solid transition in a two-component plasma has to be questioned. Apparently, the OCP-assumption of a homogeneous rigid neutralizing background gives rise to substantial deviations of the critical parameters. More simulations are underway to verify and generalize these predictions.

Acknowledgements This work has been supported by the Deutsche Forschungsgemeinschaft through SFB TR24 project A5.

References

[1] M. Bonitz, V. S. Filinov, V. E. Fortov, P. R. Levashov, and H. Fehske, Phys. Rev. Lett. **95**, 235006 (2005).
[2] M. Bonitz et al., Phys. Plasmas **15**, 055704 (2008).
[3] S. Ichimaru, H. Iyeltomi, and S. Tanaka, Phys. Rep. **149**, 91-205 (1987).
[4] T. Ott, M. Stanley, and M. Bonitz, Phys. Plasmas **18**, 063701 (2011).
[5] F. Lindemann, Z.Phys. **11**, 609, (1910).
[6] M.D. Jones and D.M. Ceperley, Phys. Rev. Lett. **76**, 4572 (1996).
[7] B. Militzer and R.L. Graham, J. Phys. Chem. Solids **67**, 2136 (2006).
[8] V.S. Filinov, M. Bonitz, and V.E. Fortov, JETP Lett. **72**, 245 (2000), [Pisma v ZhETF **72**, 361 (2000)].
[9] M. Bonitz, V.S. Filinov, V.E. Fortov. P.R. Levashov, and H. Fehske, J. Phys. A: Math. Gen. **39**, 4717 (2006); V.S. Filinov, H. Fehske, M. Bonitz, V.E. Fortov, and P.R. Levashov, Phys. Rev. E **75**, 036401 (2007).
[10] W.-D. Kraeft, D. Kremp, W. Ebeling, and G. Röpke, "Quantum Statistics of Charged Particle Systems", Akademie-Verlag Berlin 1987.
[11] W. Ebeling, W.D. Kraeft, and G. Röpke, Contrib. Plasma Phys. **52**, 7 (2012).
[12] G.E. Norman, I. Yu. Skobelev, and V.V. Stegailov, Contrib. Plasma Phys. **51**, 411 (2011).
[13] H. Haberland, M. Bonitz, and D. Kremp, Phys. Rev. E **64**, 026405 (2001).
[14] V.M. Zamalin, G.E. Norman, and V.S. Filinov, "The Monte Carlo Method in Statistical Thermodynamics" (Nauka, Moscow, 1977), (in Russian).
[15] "Introduction to computational methods for many-body physics", M. Bonitz and D. Semkat (Eds.). Rinton Press, Princeton 2006; "Computational Many Particle Physics" H. Fehske, R. Schneider, and A. Weiße (Eds.), Lecture Notes in Physics **739**, Springer Berlin Heidelberg 2008.
[16] V.S. Filinov, M. Bonitz, W. Ebeling, and V.E. Fortov, Plasma Phys. Control. Fusion **43**, 743 (2001).
[17] R.P. Feynman and A.R. Hibbs, "Quantum Mechanics and Path Integrals", McGraw-Hill, New York, Moscow 1965.

